Heat Transfer and Flow Characteristics in Impinging Flows with Turbulators

Tzeng-Yuan Chen* and Chia-Ching Li

Department of Aerospace Engineering, Tamkang University, Tamsui, Taiwan 251, R.O.C.

Abstract

The heat transfer characteristics in impinging flows with turbulators were experimentally investigated. The flow characteristics were also measured to elucidate the obtained heat transfer results. Uniform flows were generated at the inlet of a duct, and flowed out through the duct side-open slots near the duct end. A heat-transfer surface was located at the duct end, perpendicular to the incoming flow for heat transfer measurements. A pair of turbulator was mounted on the duct walls at the duct inlet, including rectangular-plate and triangular-plate turbulators, 45° and 90° angle of attacks. Temperatures on the heat-transfer surface were measured by thermocouples to obtain the average Nusselt number. Three-component mean and fluctuating velocity measurements by laser Doppler velocimetry were conducted to characterize the flow structures and to obtain the flow characteristics near the heat-transfer surface. Results show that the turbulators have the effect to increase the flow mean impinging velocity, axial vorticity and turbulent kinetic energy near the heat transfer surface and, thus, to augment the heat transfer. The 90° rectangular-plate turbulator and 45° delta-wing turbulator cause the largest and least heat transfer augmentation among the investigated turbulators, respectively.

***Key Words*:** Convective Heat Transfer, Impinging Flow, Turbulator

1. Introduction

Impinging jet flows have been widely applied in industries for heat transfer applications. For examples, the impinging jets are used to cool gas turbine blades, electronic equipments, CPU heat sinks and so on. Studies [1–5] on these topics have been conducted to understand the jet flows, the jet flow parameter effects on heat transfer, and to investigate the heat transfer enhancement by turbulators. For examples, Lytle and Webb [1] experimentally investigated the local heat transfer characteristics of air jet impingement at nozzle-plate spacing of less than one nozzle diameter. Their study showed that effects of accelerating fluid between the nozzle-plate gap as well as a significant increase in local turbulence leads to substantially increased local heat transfer with decreased nozzle-plate spacing. The outer peak in local Nusselt number was found to move radically outward for larger nozzle-plate spacing and higher Reynolds numbers. Fitzgerald and Garimella [2] experimentally studied the flow field of an axisymmetric, confined and submerged turbulent jet impinging normally on a flat plate. A toroidal recirculation zone was observed. The location of the center of the toroid moved radially outward, both with an increase in Reynolds number in nozzle-to-target spacing. Increasing the nozzle diameter resulted in a decrease in peak radial velocity, but an increase in peak turbulence levels. Garimella and Nenaydykh [3] experimentally studied the effect of nozzle geometry (diameter and aspect ratio) on the local heat transfer coefficients from a small heat source to an axisymmetric jet. Their study showed that at very small aspect ratios, the heat transfer coeffi-

*Corresponding author. E-mail: tychen@mail.tku.edu.tw

cients are the highest. As the aspect ratio is increased to values of 1–4, the heat transfer coefficients drop sharply, but with further increases to 8–12, the heat transfer coefficient gradually increases. They concluded that these results are possibly due to the flow separation and reattachment in the nozzle, and its effect on exit velocity profiles. Ekkad and Kontrovitz [4] investigated jet impingement heat transfer on dimpled target surfaces. Their study focused on determining whether the presence of dimples enhances heat transfer. Results showed that the presence of dimples on the target surface, in-line or staggered with respect to jet location, produce lower heat transfer coefficients than the non-dimpled target surface. Wen and Jang [5] experimentally investigated the heat transfer characteristics of impinging jets with/without swirling inserts. Their study showed that the crossed-swirling-strip insert has better heat transfer performance than the longitudinal swirling-strip insert. The percentage increase in heat transfer enhancement varied up to 14%, as the Reynolds number increases.

The previous studies have provided some insights into the flow and heat transfer characteristics in impinging jet flows. The turbulator effects on the main impinging flow structures, the near-wall flow structures and the relations between quantitative flow and heat transfer characteristics have been less investigated and discussed in literatures. In this study, the cross-sectional flow structures with and without a rectangular-plate turbulator are first investigated. The flow characteristics near the heat transfer surface, including the axial mean impinging velocity, axial vorticity and turbulent kinetic energy are then studied. Temperatures on the heat transfer surface are measured to obtain the average Nusselt number. The turbulator effects on the heat transfer and flow parameters are examined and discussed.

2. Experimental Setup and Methods

2.1 Experimental Setup

The primary experimental setup utilized in this research is shown in Figure 1. An open-circuit wind tunnel system was used to develop uniform flows with turbulence intensities less than 1 percent. Air was supplied by a blower, and passed through a turbulence-management section that includes a diffuser, honeycombs, screens and a contraction section, to a 7×7 cm^2, 25 cm long duct. The air flowed out the duct through the two side openings of 3.5×7 cm^2, located at the duct end, see Figure 2. A 4×4 cm^2 heat transfer plate was located at the bottom end of the duct, perpendicular to the incoming flow, for heat transfer measurements. A pair of turbulators was placed at the duct inlet. Four types of turbulators were used in this study, including delta-wing and rectangular-wing turbulators with 45° and 90° angle of attacks. The base width and tip height of the turbulators are 7 and 1.5 cm, respectively. The origin of the coordinate system used for data presentation is at the center of the heat-transfer plate. The investigated flows include the flows with and without turbulators, and the Reynolds numbers are between 4400 and 30800 based on the duct hydraulic diameter.

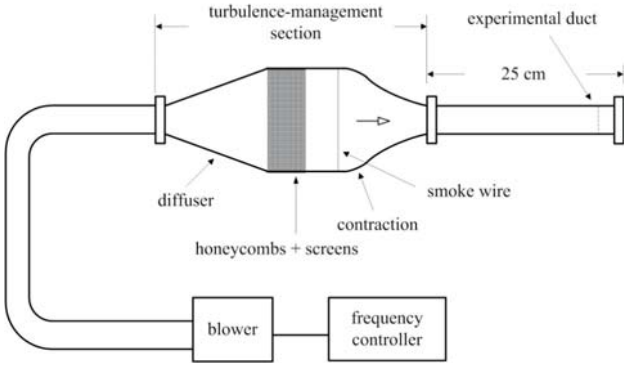

Figure 1. The primary experimental setup.

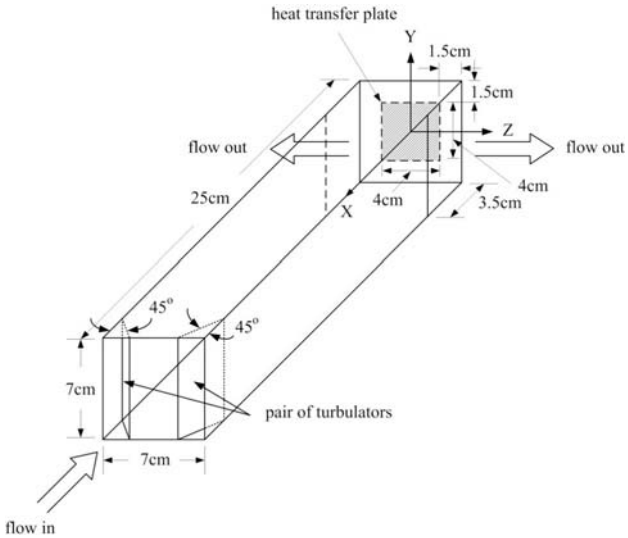

Figure 2. The experimental duct, showing the flow conditions, the locations of turbulators, heat-transfer plates, and the coordinate system.

2.2 Velocity Measurement

Three-component, mean and fluctuating velocity measurements were performed under isothermal conditions using TSI laser Doppler velocimetry (LDV). The LDV includes a 4*W* Argon-ion laser, transmitting optics, a frequent shift system, receiving optics, a Colorlink system and an IFA650 digital burst correlator. The ellipsoidal probe volume produced by the transmitting optics is 0.137 mm in diameter and 1.408 mm in length with fringe spacing of 2.67 μm. Each velocity is calculated from 4096 collected velocity samples. The mean velocity ($\bar{v}$) is the average value of the 4096 velocity samples and the fluctuating velocity is obtained from $\sqrt{\sum v^2 / 4096 - \bar{v}^2}$, where v is the local instant velocity. A smoke wire, located upstream of the apparatus, was used to generate particles for the LDV measurements, and the data rates are in the order of hundreds. These measurements were conducted at duct cross-sections to characterize the flow structures, and near the heat-transfer surface to obtain the flow parameters, including the mean impinging velocity, axial vorticity and turbulent kinetic energy. These flow parameters were obtained from 64 velocity data measured at 7 mm away from the heat transfer surface, as indicated in Figure 3. The uncertainty in the measured velocity ranges was less than 5 percent from the repeatability tests conducted during the test runs.

2.3 Heat Transfer Measurement

The heat transfer coefficient, $h = \dfrac{Q_{in} - Q_{loss}}{A(T_w - T_0)}$, was measured on the heat transfer surface, which consists of a copper plate, an electrical insulation plate, a heating plate, and a fiberglass plate, see Figure 3. Electrical power, Q_{in}, of 3-8W was supplied to the heating plate from a *DC* power supply, resulting in a constant-heat-flux heat-transfer surface. The reference temperature, T_0, is the air inlet temperature, obtained using a Type-T, 0.1 mm-diameter thermocouple placed at the duct inlet, which is approximate the room temperature of 23 °C. This research investigated the turbulator effects on the overall heat transfer characteristics of the heat transfer surface. Due to the high conductivity of the copper plate, the temperatures on the heat transfer surface differ little. Thus, nine thermocouples only were installed beneath the copper plate to evaluate the average heat-transfer surface temperature, T_w, and the conduction and radiation heat losses, Q_{loss}. The average surface temperatures were in the range of 55 °C to 85 °C for the investigated 45 flow conditions with the uncertainty of 1 °C from repeatability tests. The heat conduction loss through the back of the heating plate was calculated using Fourier's law by knowing the temperature drop, which is less than 2.7 percent of the power input. Radiation loss was estimated to be less than 4 percent of the power input. The natural convection was neglected in the present study because the values of Gr_L/Re_L^2 are much smaller than 1 on the heat transfer surface, where Gr_L and Re_L are the Grashof number and Reynolds number, respectively, based on the characteristic length of the heat transfer plate. The temperatures were read using a TempScan/1100 system produced by IOtech, Inc, with the uncertainty within 0.5 °C.

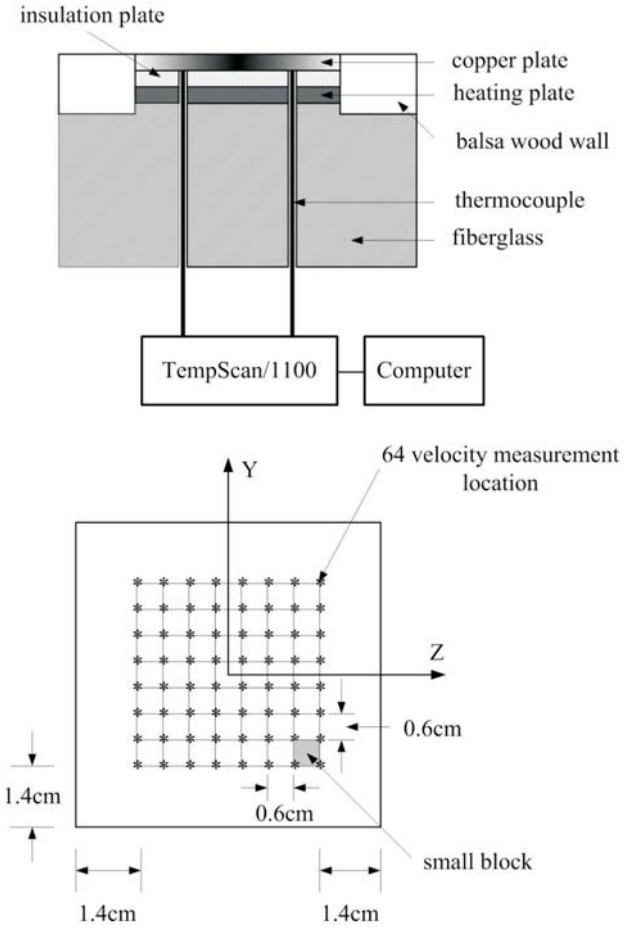

Figure 3. Near heat-transfer surface velocity measurement locations and a schematic of the heat-transfer surface.

The uncertainty in heat transfer measurement was estimated to be within 8 percent.

3. Results and Discussion

3.1 Cross-sectional Flow Structures

The duct cross-sectional flow velocities for the investigated flows were discussed first to characterize the overall flow structures. Figures 4–6 present the typical features of the velocity vectors in duct central plane (*X*-*Y* plane, *Z* = 0) for flows of Reynolds number 17600 without and with turbulators. Figure 4 shows that the flow is generally symmetric about the duct central plane, and behaves similar to a stagnation flow at the heat transfer surface. The flow decelerates along the duct central plane and accelerates out of the duct from the side slots. The pair of 45° delta-wing turbulators causes the flow recirculated behind the turbulators, as shown in Figure 5. The flow is still generally symmetric, and the axial velocities (X-component) in the central region are slightly larger than those for the flow without the turbulator as the result of the recirculated flow. The mean flow structure near the heat transfer surface is basically similar to that without the turbulator. Figure 6 shows that the 90° rectangular turbulators largely disturb the flow, resulting in a non-symmetric flow structure. The recirculating flow region on the left side is much larger than that on the right side. This asymmetric flow behavior has been observed in sudden flow as discussed by Cherdron et al. [6]. The result also possibly lies in disturbances generated at the edge of the vortex generators and amplified in the shear layers, and a shedding of eddy-like patterns alternate from one side to the other with consequent asymmetry of the mean flow, particularly of the dimensions of the two regions of recirculation.

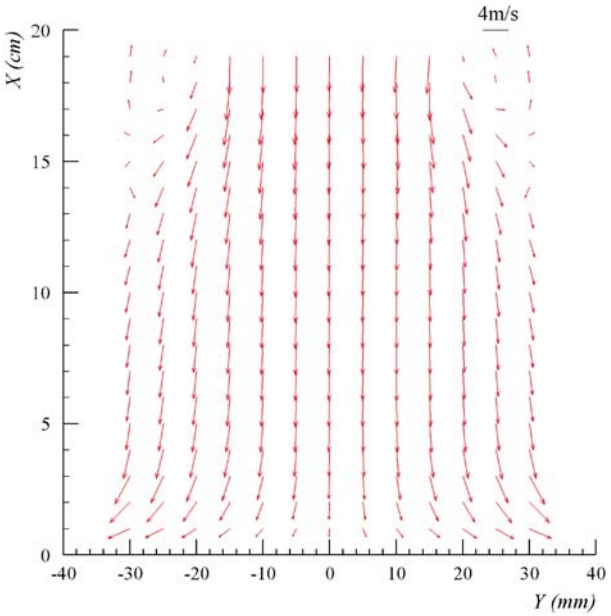

Figure 5. The flow structure in duct central plane (X-Y plane, Z = 0) for the flow with 45° delta-wing turbulator.

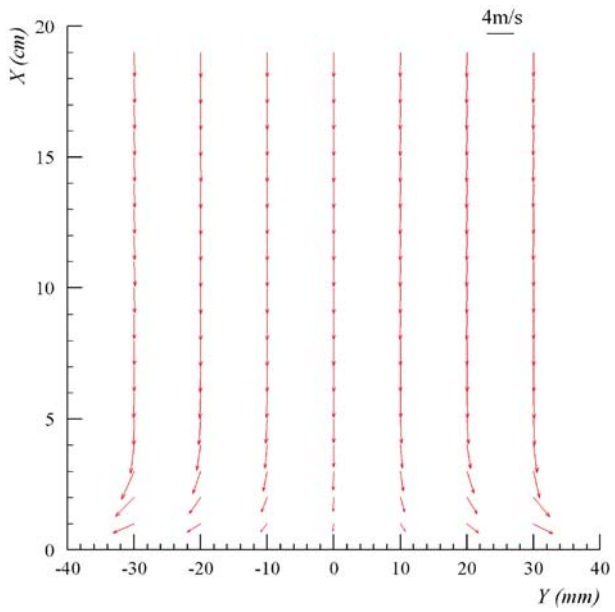

Figure 4. The flow structure in duct central plane (X-Y plane, Z = 0) for the flow without turbulator.

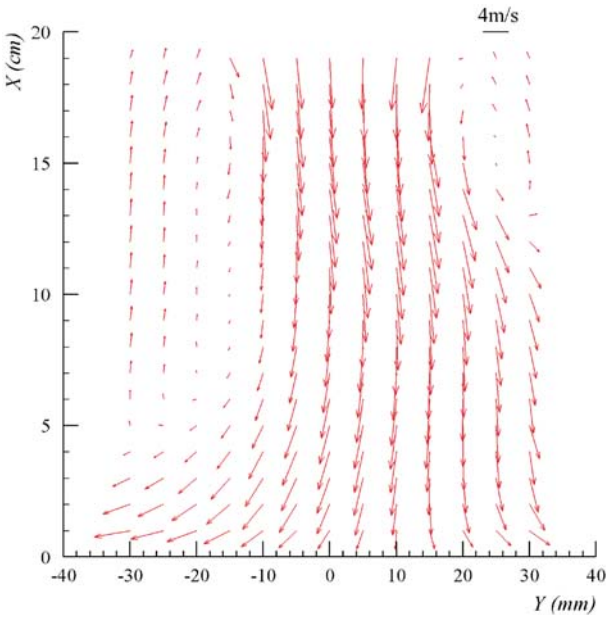

Figure 6. The flow structure in duct central plane (X-Y plane, Z = 0) for the flow with 90° rectangular turbulator.

3.2 Flow Characteristics Near Heat Transfer Surface

The velocity field near the heat transfer surface has major effects on heat transfer process. Three flow parameters near the heat transfer surface, including the mean impinging velocity (U_{ave}), the axial vorticity (η) and the turbulent kinetic energy are determined. These flow parameters were obtained from sixty-four, three component velocities, measured at 7 mm from the heat transfer surface. The mean impinging velocity is the averaged value of the 64, X-component, mean velocities. The axial vorticity is the averaged value of the 49-block vorticity, where the vorticity of each block is obtained from the Y-, and Z-component mean velocities at block corners. The turbulent kinetic energy, $(u'^2 + v'^2 + w'^2/2)^{1/2}$, is calculated from the 64, X-, Y- and Z-component fluctuating velocities.

3.2.1 Mean Impinging Velocity

The impinging velocity is an indication of impinging effect on heat transfer. Its magnitude is expected to be proportional to the heat transfer rate. Figure 7 presents the distributions of the normalized mean impinging velocity with Reynolds number for some of the test conditions. The normalized mean impinging velocity (U_{ave}/U_d, where U_d is the duct average velocity) is, in general, invariant with the Reynolds number. The turbulators increase the mean impinging velocity, especially the 90° rectangular turbulator. As noted in Figures 4–6 that the turbulators resulted in the flow recirculation. The flow would accelerate in the central flow region to maintain the constant flow rate. The recirculation region is the largest for the flow with the 90° rectangular turbulator among the test flow conditions, and thus, the mean impinging velocity is also the largest. The increase in the mean impinging velocity is up to 100% and 50% for the flows with the 90° rectangular turbulator and the 45° delta-wing turbulator, respectively.

3.2.2 Axial Vorticity

Large strength of the secondary flow should have a large effect on heat transfer augmentation. Figure 8 presents the distributions of normalized axial vorticity ($\eta D/U_d$, where D is the duct hydraulic diameter) with Reynolds number for some of the test conditions. This figure indicates that the turbulators increase the strength of the secondary flow near the heat-transfer surface, especially the 90° rectangular turbulator. As noted in Figures 4–6 that the 90° rectangular turbulator largely disturbs the flow, and results in large flow velocity variations, while the 45° delta-wing turbulator does not largely disturb the flow except in the flow recirculation region. The axial vorticities for the flow with the 90° rectangular turbulator are, thus, much larger than the other two test conditions.

3.2.3 Turbulent Kinetic Energy

Large turbulent kinetic energy is expected to have a large effect on heat transfer augmentation. Figure 9 presents the distributions of normalized turbulent kinetic energy with Reynolds number for some test flow conditions. Since the turbulators disturb the flow and increase

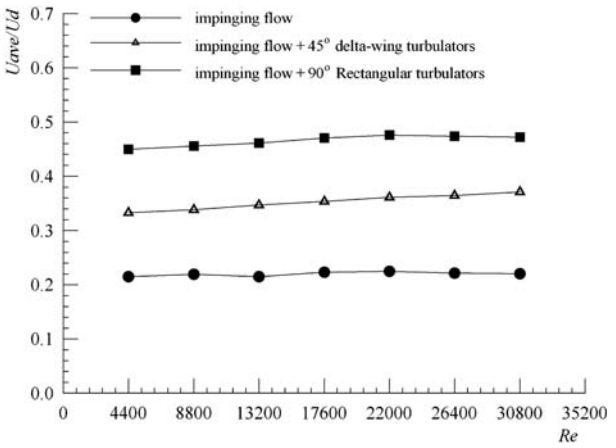

Figure 7. The distributions of normalized mean impinging velocity with Reynolds number.

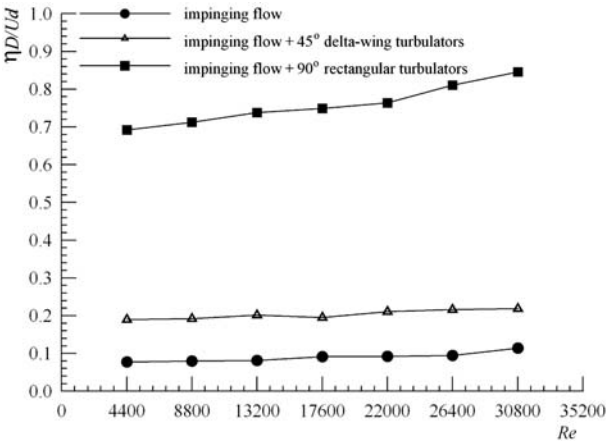

Figure 8. The distributions of normalized axial vorticity with Reynolds number.

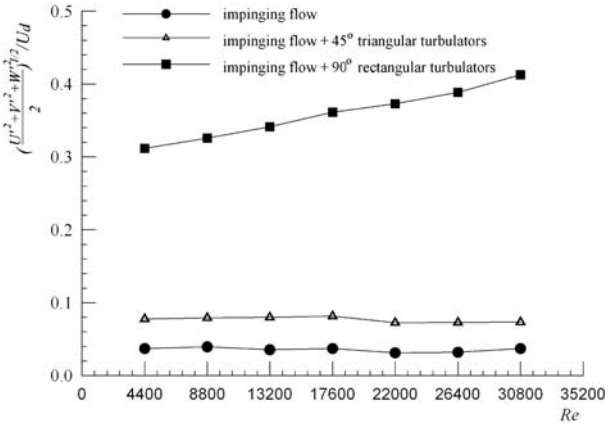

Figure 9. The distributions of normalized turbulent kinetic energy with Reynolds number.

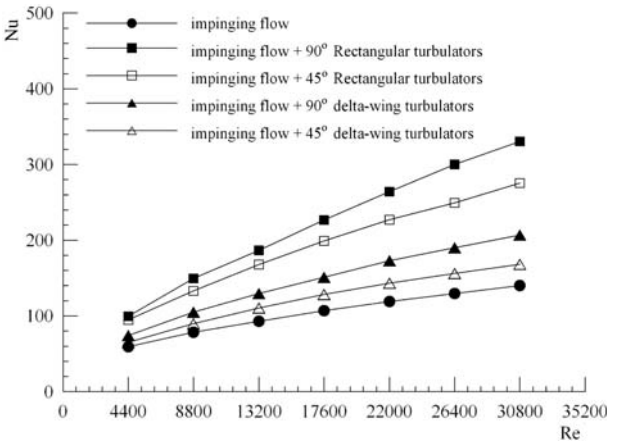

Figure 10. The distributions of average Nusselt number with Reynolds number under constant flow velocity condition.

the flow unsteadiness, the turbulent kinetic energy is, accordingly, increased by the turbulators, especially for the 90° rectangular turbulator.

3.3 Heat Transfer Results

The heat transfer studies were performed under constant flow velocity and constant pumping power conditions. The insertion of turbulators into the duct causes pressure losses in the flow. Thus, for constant flow velocity tests, the power inputs to the blower for the tests with turbulators should be adjusted in order that the flow velocities for the flows with turbulators are the same as that for the flow without turbulator. For constant pumping power tests, the power inputs to the blower for the flows with turbulators are the same as that without turbulator. In this case, the flow velocities for the flow with turbulators are smaller than that for the flow without turbulator. Figure 10 presents the distributions of the averaged Nusselt number on the heat transfer surface with Reynolds number for the five test conditions, showing that the Nusselt number increases with Reynolds number, as expected. The 90° rectangular turbulator and 45° delta-wing turbulator have the largest and least heat transfer augmentation among the test conditions. Also, the turbulator has larger effect on heat transfer augmentation with larger Reynolds number. The augmentation is 135% and 68% for the case with 90° rectangular turbulator of Reynolds numbers 30800 and 4400, respectively, and is 20% and 10% for the case with 45° delta-wing turbulator of Reynolds number 30800 and 4400, respectively. The distributions of the averaged Nusselt number on the heat transfer surface with Reynolds number for the constant pumping power test condition are presented in Figure 11. The Nusselt number distributions are qualitatively similar to those for the constant flow velocity condition, but with less heat transfer augmentation. The heat transfer augmentation is up to 93% for the case with 90° rectangular turbulator of Reynolds numbers 30800, and is 15% for the case with 45° delta-wing turbulator of Reynolds number 30800.

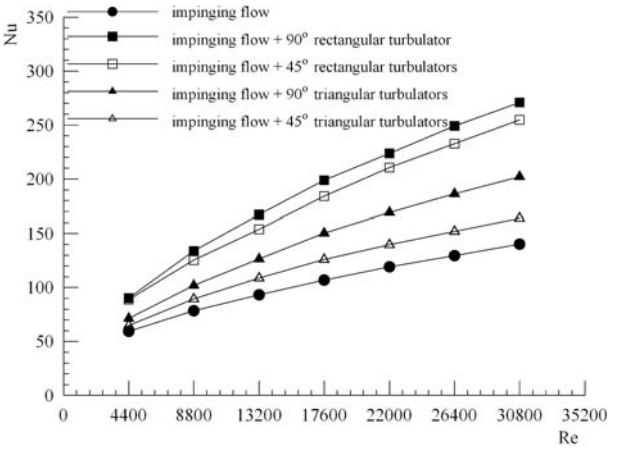

Figure 11. The distributions of average Nusselt number with Reynolds number under constant pumping power condition.

It has been shown above that the turbulators have the effect to increase the mean impinging velocity, axial vorticity and turbulent kinetic energy, and to augment heat transfer. This study further confirms that the heat transfer rate is proportional to the impinging velocity, the strength of the vorticity and the degree of flow turbulence. Figures 7–9 have shown that the 90° rectangular tur-

bulator causes the largest increases in mean impinging velocity, axial vorticity and turbulent kinetic energy, and thus, results in the largest heat transfer augmentation among the test turbulators.

4. Conclusion

Results of this study indicate that the turbulators in impinging flows increase the mean impinging velocity, axial vorticity and turbulent kinetic energy near the heat transfer surface, and augment heat transfer for the investigated Reynolds numbers. The 90° rectangular turbulator results in the largest heat transfer augmentation among the test turbulators. The reasons are due that the 90° rectangular turbulator causes large flow recirculation region, and thus, causes the largest increases in mean impinging velocity, axial vorticity and turbulent kinetic energy near the heat transfer surface.

References

[1] Lytle, D. and Webb, B. W., "Air Jet Impingement Heat Transfer at Low Nozzle-plate Spaceing," *Int. J. Heat Mass Transfer,* Vol. 37, pp. 1687–1697 (1994).

[2] Fitzgerald, J. A. and Garimella, S. V., "A Study of the Flow Filed of a Confined and Submerged Impinging Jet," *Int. J. Heat Mass Transfer,* Vol. 41, pp. 1025–1034 (1998).

[3] Garimella, S. V. and Nenaydykh, B, "Nozzle-Geometry Effects in Liquid Jet Impingement Heat Transfer," *Int. J. Heat Mass Transfer,* Vol. 39, pp. 2915–2923 (1996).

[4] Ekkad, S. V. and Kontrovitz, D, "Jet Impingement Heat Transfer on Dimpled Target Surfaces," *Int. J. of Heat and Fluid Flow,* Vol. 23, pp. 22–28 (2002).

[5] Wen, M. Y. and Jang, K. J., "An Impingement Cooling on a Flat Surface by Using Circular Jet with Longitudinal Swirling Strips," *Int. J. Heat Mass Transfer,* Vol. 46, pp. 4657–4667 (2003).

[6] Cherdron, W., Durst, F. and Whitelaw, J. H., "Asymmetric Flows and Instabilities in Symmetric Ducts with Sudden Expansions," *J. Fluid Mechanics,* Vol. 84, pp. 13–31 (1978).

Manuscript Received: Oct. 6, 2005
Accepted: Apr. 28, 2006